FULL PAPER

BJC

British Journal of Cancer (2017) 117, 233–244 | doi: 10.1038/bjc.2017.164

Keywords: hepatocellular carcinoma; microRNA; N-cadherin; EMT; Akt

MicroRNA-199b-5p attenuates TGF-β1-induced epithelial–mesenchymal transition in hepatocellular carcinoma

Shao-jun Zhou[1], Fu-yao Liu[2], An-hong Zhang[3], Hui-fang Liang[4], Ye Wang[3], Rong Ma[1], Yuan-hui Jiang*[,3] and Nian-feng Sun*[,1]

[1]Department of General Surgery, Qilu Hospital of Shandong University, 107 West Culture Road, Jinan 250012, China; [2]Department of Gastrointestinal Medical Oncology, Division of Cancer Medicine, The University of Texas MD Anderson Cancer Center, 7455 Fannin Street, Houston, Texas 77054, USA; [3]Department of General Surgery, Qilu Hospital of Shandong University, 758 Hefei Road, Qingdao 266035, China and [4]Research Laboratory and Hepatic Surgery Center, Department of Surgery, Tongji Hospital, Tongji Medical College, Huazhong University of Science and Technology, 1095 Jie Fang Da Dao, Wuhan 430030, China

Background: Accumulating evidence indicates that N-cadherin is a cell adhesion molecule that has critical roles in tumour progression. However, the role of N-cadherin in hepatocellular carcinoma (HCC) remains controversial.

Methods: This study aims to investigate the expression status of N-cadherin and its molecular mechanisms in HCC.

Results: The expression of N-cadherin was markedly overexpressed in HCC tissues and cell lines. We identified that miR-199b-5p binds to the 3′-UTR of N-cadherin mRNA, thus decreasing N-cadherin expression in HCC cells. We also found the downregulation of miR-199b-5p in HCC specimens, which was inversely correlated with N-cadherin upregulation, predicted poor clinical outcomes in HCC patients. Next, we determined that miR-199b-5p overexpression promoted cell aggregation, suppressed cell migration and invasion in HCC cells, and inhibited xenografts tumour metastasis in nude mice. Moreover, we demonstrated that miR-199b-5p attenuated TGF-β1 induced epithelial–mesenchymal transition (EMT) -associated traits, while its effects could be partially reversed by N-cadherin restoration. Finally, we examined that N-cadherin downregulation or miR-199b-5p overexpression suppressed TGF-β1-induced Akt phosphorylation, and inhibition of PI3K/Akt pathway blocked TGF-β1-induced N-cadherin overexpression in HCC cells.

Conclusions: Our data demonstrate that N-Cadherin was markedly overexpressed and miR-199b-5p was significantly downregulated in HCC. MiR-199b-5p exerts inhibitory effects on EMT, and directly targets N-cadherin in HCC, supporting the potential utility of miR-199b-5p as a promising strategy to treat HCC. Also, a positive regulatory loop exists between N-cadherin and Akt signalling represents a novel mechanism of TGF-β1-mediated EMT in HCC cells.

Hepatocellular carcinoma (HCC) is the fifth most common cancer and the third most common cause of cancer related deaths worldwide (El-Serag and Rudolph, 2007). HCC patients face a high incidence of recurrence when receiving curative therapy for early stage HCC due to invasion and metastasis (El-Serag *et al*, 2008). Therefore, molecular mechanisms underlying HCC invasion, metastasis and recurrence deserve further investigation to develop new prognostic biomarkers and novel therapeutics for HCC patients.

Emerging evidence indicates that epithelial–mesenchymal transition (EMT), especially TGF-β1-mediated crucial pathway and distinct processes, such as loss of cell–cell contacts, disruption

*Correspondence: Professor Y-h Jiang; E-mail: jyh2@sina.com or Professor N-f Sun; E-mail: sunnianfeng@126.com

Received 12 January 2017; revised 4 April 2017; accepted 16 May 2017; published online 6 June 2017

of cell polarity, matrix remodelling, migration and invasion has a pivotal role in HCC progression through cumulative genetic and epigenetic alterations (Lamouille *et al*, 2014). EMT neoplastic cells manifest with increased motility, invasion, mesenchymal characteristics and metastatic potential, along with the loss of E-cadherin expression, the upregulation of N-cadherin and other EMT-related factors (Hanahan and Weinberg, 2011; Nieto *et al*, 2016). The role of E-cadherin in tumour invasion and metastasis has been well established in cancers (Umbas *et al*, 1994; Nass *et al*, 2000; Bremnes *et al*, 2002). However, the role of N-cadherin in HCC remains to be elucidated. N-cadherin is reported highly expressed in multiple cancers, such as breast cancer, prostate cancer, melanoma and so on (Hazan *et al*, 2000; Li *et al*, 2001; Gravdal *et al*, 2007). Accumulating evidence suggests its role in carcinogenesis, but the molecular mechanisms underlying aberrant N-cadherin expression in HCC remain elusive.

Micro-RNAs (miRNAs) are small non-coding RNAs that interact with the 3′-untranslated region (3′-UTR) of target mRNAs and repress expression by inhibiting translation or inducing degradation (Kim, 2005). It has been reported that miRNAs perform pleiotropic functions to modulate key cellular processes involved in carcinogenesis (Calin and Croce, 2006; Croce, 2009; Liu *et al*, 2015). Recent studies revealed that various miRNAs are involved in regulating EMT in cancer cells. TGF-β1 promoted EMT-related carcinogenesis by inducing miR-181b expression and ectopic expression of miR-630 attenuated the TGF-β1-activated EMT process (Wang *et al*, 2015; Chen *et al*, 2016). Given the pivotal roles of EMT in tumour invasion, metastasis and recurrence, identification of key candidate miRNAs could be further investigated as potential biomarkers or therapeutic targets.

In this study, we explored the expression pattern of N-cadherin in HCC and its clinical significance, and we identified that miR-199b-5p binds to the 3′-UTR of N-cadherin via targeting N-cadherin. The role and function of miR-199b-5p in carcinogenesis and EMT was further investigated.

MATERIALS AND METHODS

Patients and specimens. One hundred pairs of human HCC tissues and their corresponding adjacent liver tissues were collected from patients who underwent liver resection between January 2010 and May 2011 at the Hepatic Surgery Center of Huazhong University of Science and Technology (HUST). Informed consent was obtained from all the patients before participating in the study, which was approved by the medical ethics committee of Tongji Hospital, HUST, China.

Micro-RNAs, plasmids and materials. MiR-199b-5p mimics and inhibitors, and N-cadherin siRNA were purchased from RiboBio Co., Ltd (Guangzhou, China). The hsa-miR-199b-5p expressing plasmid and negative control plasmid were synthesised by GeneChem (Shanghai, China). Full-length 3′-UTR of N-cadherin was purchased from GeneChem, amplified by PCR, and cloned into the pMIR-REPORT luciferase expression vector (Ambion, Austin, TX, USA) as a Luc-UTR vector. Mutated miR-199b-5p target sequences of N-cadherin 3′-UTR in the Luc-MUT vector were conducted using site-directed mutagenesis (Stratagene, La Jolla, CA, USA). Full-length N-cadherin was purchased from GeneChem and cloned into pcDNA3.1 (+) expression vector (Invitrogen, Carlsbad, CA, USA). (Phosphatidylinositol 3-kinase) PI3K inhibitor LY294002 (SelleckChemicals, Houston, TX, USA) were dissolved in DMSO to a concentration of 20 μM. Akt Inhibitor VIII (Akti VIII) were dissolved in DMSO to a concentration of 5 μM. TGF-β1 receptor kinase inhibitor SB431542 (SelleckChemicals) were dissolved in DMSO to a concentration of 10 μM. TGF-β1 (Sigma-Aldrich, St Louis, MO, USA) were dissolved in PBS and 10 mM citric acid to a concentration of 5 ng ml^{-1} for usage.

Cell culture and transfection. Human HCC cell lines BEL7402, Hep3B, HepG2, HLF, Huh7 and normal liver cell line HL7702 were purchased from Typical Training Content Preservation Committee Cell Bank, Chinese Academy of Sciences (Shanghai, China). The cells were maintained in Dulbecco's modified Eagle's medium (DMEM; Gibco; Thermo Fisher Scientific, Waltham, MA, USA) supplemented with 10% fetal bovine serum (FBS; Gibco; Thermo Fisher Scientific) and penicillin/streptomycin (100 U ml^{-1}) at 37 °C in humidified atmosphere with 5% CO_2. Cells were transfected using Lipofectamine 2000 (Invitrogen) following the manufacturer's protocol. For stable transfections, 5×10^5 cells were seeded in a six-well plate. The hsa-miR-199b-5p expressing plasmid and negative control plasmid were transfected into the cells for 48 h. And cells were trypsinised, resuspended and seeded in a six-well plate (100 cells per well). Afterwards, cells were cultured in DMEM containing 10% FBS and 500 μg ml^{-1} of G418 (Calbiochem, Darmstadt, Germany) for 3 weeks. The positive cell clones were isolated, cultured and determined using western blotting assay.

***In silico* analysis.** To investigate whether miRNAs were involved in regulating N-cadherin expression in HCC, we utilised mirwalk database (http://zmf.umm.uni-heidelberg.de/apps/zmf/mirwalk/micrornapredictedtarget.html), which integrated four commonly used miRNA databases (TargetScan, Pictar, miRwalk and miRanda), to scan for the potential miRNAs that may target 3′-UTR of N-cadherin mRNA (Dweep *et al*, 2011).

RNA isolation and quantitative real-time PCR (qRT-PCR) assays. Total RNAs from both tissues and cells were extracted using Trizol reagent (Invitrogen). MiR-199b-5p was reverse transcribed using ReverTra Ace qPCR RT Kit (TOYOBO, Osaka, Japan) and was measured using SYBR Green Realtime PCR Master Mix (TOYOBO) via StepOne Real-Time PCR System (Applied Biosystems, Foster City, CA, USA). U6 RNA was used as a miRNA endogenous control. Relative expression analysis was performed using the comparative CT method ($2^{-\Delta\Delta CT}$). All experiments were performed in triplicate.

HCC EMT Cell Model and immunofluorescence assay. HepG2 and Huh7 cells were trypsinised and seeded in six-well plates and incubated for 24 h. Then the cells were treated in 2.5% FBS-containing DMEM with 5 ng ml^{-1} TGF-β1 (Sigma-Aldrich) or 5 ng ml^{-1} bovine serum albumin (BSA) (Sigma-Aldrich) used as the control for 2 days. The processed cells were washed with PBS, and fixed in 4% paraformaldehyde (Beijing Solarbio Corporation, Beijing, China), Then 0.3% TritonX-100 (Beijing Solarbio Corporation) were added for 10 min and 5% BSA 500 μl were added for 1 h at room temperature. N-cadherin antibody diluted by 5% BSA was added and then the cells were incubated at 4 °C overnight. Phycoerythrin-labelled secondary antibody (Abcam Company, Hong Kong) diluted by 5% BSA (1 : 1000) were added and the cells were incubated at room temperature in dark for 1 h. Representative images were obtained from the Nikon Digital ECLIPSE C1 system (Tokyo, Japan).

Luciferase reporter assay. To verify the target sites of miR-199b-5p, HepG2 and Huh7 cells were co-transfected with miR-199b-5p mimics or inhibitors and luciferase reporter constructs containing wild-type or mutated N-cadherin 3′-UTR. Cells were split and luciferase activities were measured using Dual-Luciferase Assay Kit (Promega, Madison, WI, USA).

Wound-healing assay and Transwell assay. Cells were seeded at a density of 4×10^5 cells per well in a six-well plate and were incubated for 24 h, followed by maintained in serum-free DMEM until the cells were grown as a confluent monolayer. Then cell migration initiated while cell layer was scratched. The migration

abilities were determined by relative gap distance. For Transwell cell migration assay, the cells were resuspended in serum-free DMEM. Then 5×10^4 cells were seeded on the upper side of a Transwell chamber (24-well insert, 8 μm pore size; Corning Costar, Cambridge, MA, USA), followed by adding 500 μl DMEM containing 10% FBS to the lower chambers. For Transwell cell invasion assay, chamber membrane was pre-coated with 30 μl BD Matrigel (BD, Franklin Lakes, NJ, USA). Then 1×10^5 cells were seeded on the upper side, and 500 μl DMEM containing 10% FBS was added to the lower chambers. After 24 h for migration or 48 h for invasion, the cells were fixed, stained and counted by the Image-Pro Plus (IPP) v6.0 software (Media Cybernetics Inc., Rockville, MD, USA). Representative images were obtained from the Nikon Digital ECLIPSE C1 system.

CCK-8 assay. Transfected and control cells (2000 per well) were seeded in a 96-well plate and incubated at 37 °C. Cell viability was analysed at 24, 48 and 72 h using Cell Counting Kit-8 (CCK-8; Dojindo, Kumamoto, Japan) according to the manufacturer's protocols.

Analysis of clonogenicity *in vitro*. For colony formation assay, transfected and control cells (500 per well) were seeded in a six-well plate and incubated at 37 °C for 14 days. The plates were fixed in 4% paraformaldehyde, stained with 0.1% crystal violet in 20% methanol. Anchorage-independent cell growth was determined by soft agar colony formation assay. Transfected and control cells (500 per well) were seeded in a six-well plate containing 0.3% noble agar and grown for 14 days. The number of colonies was determined by direct counting using an inverted microscope (Nikon).

Cell cycle and apoptosis analysis. For cell cycle analysis, 1×10^5 cells per well were seeded in the six-well plates and incubated at 37 °C for 24 h. Then cells were harvested and fixed in 70% ethanol at 4 °C overnight. Before the analysis, the cells were treated with propidium iodide containing RNase A (KeyGen Biotech. Co. Ltd., Nanjing, China) for 30 min at 37 °C. Cell cycle analysis was performed using a FACS Calibur flow cytometer (BD). For apoptosis analysis, 1×10^5 cells per well were seeded in the six-well plates and incubated at 37 °C for 48 h. Then floating and adherent cells were harvested, washed and stained for 15 min with Annexin V-fluorescein isothiocyanate, PE (Phycoerythrin) and 7-AAD (7-amino-actinomycin D) in 500 ul binding buffer and then analysed by flow cytometry.

Cell aggregation assay. Transfected and control cells were washed, and detached with 0.05% trypsin containing 0.5 mM Ca^{2+}. Then the cells were washed with HCMF buffer (10 mM HEPES (pH 7.4), 0.137 M NaCl, 5.4 mM KCl, 0.34 mM Na_2HPO4, $12H_2O$ and 0.1% glucose), and resuspended at 2×10^5 cells per ml HCMF buffer. A total of 2×10^5 cells in 1 ml HCMF buffer containing 1 mM Ca^{2+} were seeded in the 12-well plate that was pre-coated with BSA, and kept rotating at 80 r.p.m. for 1 h at 37 °C. Cells were fixed, counted and the aggregation index (total number of aggregates and single cells/total cell number) was calculated (Huang *et al*, 2003).

Western blotting assay. Total proteins were extracted from HCC tissues and cells, and their concentrations were measured using a Pierce BCA Protein Assay Kit (Thermo Fisher Scientific). Western blotting assay was conducted using specific primary antibodies against Snail, Slug (1 : 1000; Santa Cruz Biotechnology, Dallas, TX, USA), E-Cadherin, Akt, phosphorylated Akt (p-Akt) (1 : 1000; Epitomics, Burlingame, CA, USA), N-Cadherin (Thermo Fisher Scientific), Smad2, p-Smad2, Smad3, Smad4 and GAPDH (1 : 1000; Abcam) and appropriate horseradish peroxidase-conjugated secondary antibodies (1 : 5000; Thermo Fisher Scientific). Protein bands were visualised using an enhanced chemiluminescence detection system (Thermo Fisher Scientific). The average grey scale intensities were measured by IPP v6.0 software (Media Cybernetics Inc.).

Immunohistochemistry. Immunohistochemical staining was performed according to the instructions using the following appropriate antibodies mentioned above. The results were assessed independently by two pathologists.

Xenograft assay. Twenty 4-week-old male BALB/c athymic nude mice were purchased from Chinese Academy of Medical Sciences Institute of experimental animals (Beijing, China) and bred under pathogen-free conditions at the Experimental Animal Center of Tongji Medical College. All of the animal experiments met the National Institutes of Health guidelines (NIH publication 96-01, 1996 revision) and were approved by the Committee on the Ethics of Animal Experiments of the Tongji Medical College, HUST (Permit number: SYXK (e) 2010-0057, No.00122869).

To establish intraperitoneal tumour model, TGF-β1 induced exponentially growing stably transfected miR-199b-5p and control HepG2 cells for 48 h. Then cells were suspended in DMEM (1×10^7 cells per ml), and we injected each mouse intraperitoneally with 100 μl ($n = 5$ each group). After 3 weeks, the mice were killed. Tumour nodules > 0.5 mm on the liver surface were counted. Tumour tissues were fixed in 4% formaldehyde and stored in -80 °C at the same time.

Statistical analysis. All the results were expressed as mean ± s.d. Categorical variables were compared using the χ^2-test, Fisher's exact test or one-way ANOVA with $P < 0.05$ considered statistically significant. Disease-free survival (DFS) and overall survival (OS) were calculated by the Kaplan–Meier method and compared between the groups using the log-rank test. All the experimental data were analysed using SPSS statistical software (version 16.0, Chicago, IL, USA).

RESULTS

N-cadherin is overexpressed in HCC tissues and is associated with poor clinical outcomes. N-cadherin expression was detected using immunohistochemical analysis in 100 pairs of HCC patients' tumour tissues and corresponding adjacent liver tissues. In HCC tissues, strong and homogeneous membranous staining was frequently observed (61%) at the cell–cell borders of hepatocytes, which indicated a strong positive expression of N-cadherin. Meanwhile, weak expression of N-cadherin was found in most non-cancerous liver tissues. Western blotting assay confirmed the expression patterns of N-cadherin in the HCC and adjacent liver tissues (Figure 1A). Representative images of N-cadherin expression was shown in HCC tissues and adjacent non-cancerous liver tissues (Figure 1B). Relative expression levels of N-cadherin in HCC cell lines was overexpressed compared with normal liver cell line HL7702 using western blotting assay (Figure 1C). To further investigate whether the N-cadherin expression is correlated with the prognosis of HCC patients, we found that HCC patients with high N-cadherin levels had a significantly shorter median DFS and OS compared with those with low N-cadherin levels ($P < 0.001$, Figure 1D). Moreover, the correlation between N-cadherin expression and clinicopathological features in HCC patients was assessed. N-cadherin overexpression was significantly correlated with the poor tumour differentiation, multifocal tumours of HCC, and vascular invasion ($P < 0.05$, Table 1).

N-cadherin is a direct target of miR-199b-5p in HCC cells. To investigate whether miRNAs were involved in regulating N-cadherin expression, we identified the potential miRNAs that target 3′-UTR of N-Cadherin mRNA. As a result, 8 miRNAs (hsa-miR-26a, hsa-miR-26b, hsa-miR-199-5p, hsa-miR-190, hsa-miR-204, hsa-miR-211, hsa-miR-218 and hsa-miR-369-3p) were selected out (Figure 2A). On the basis of the analysis, we transiently transfected the eight miRNAs mimics into HepG2 cell

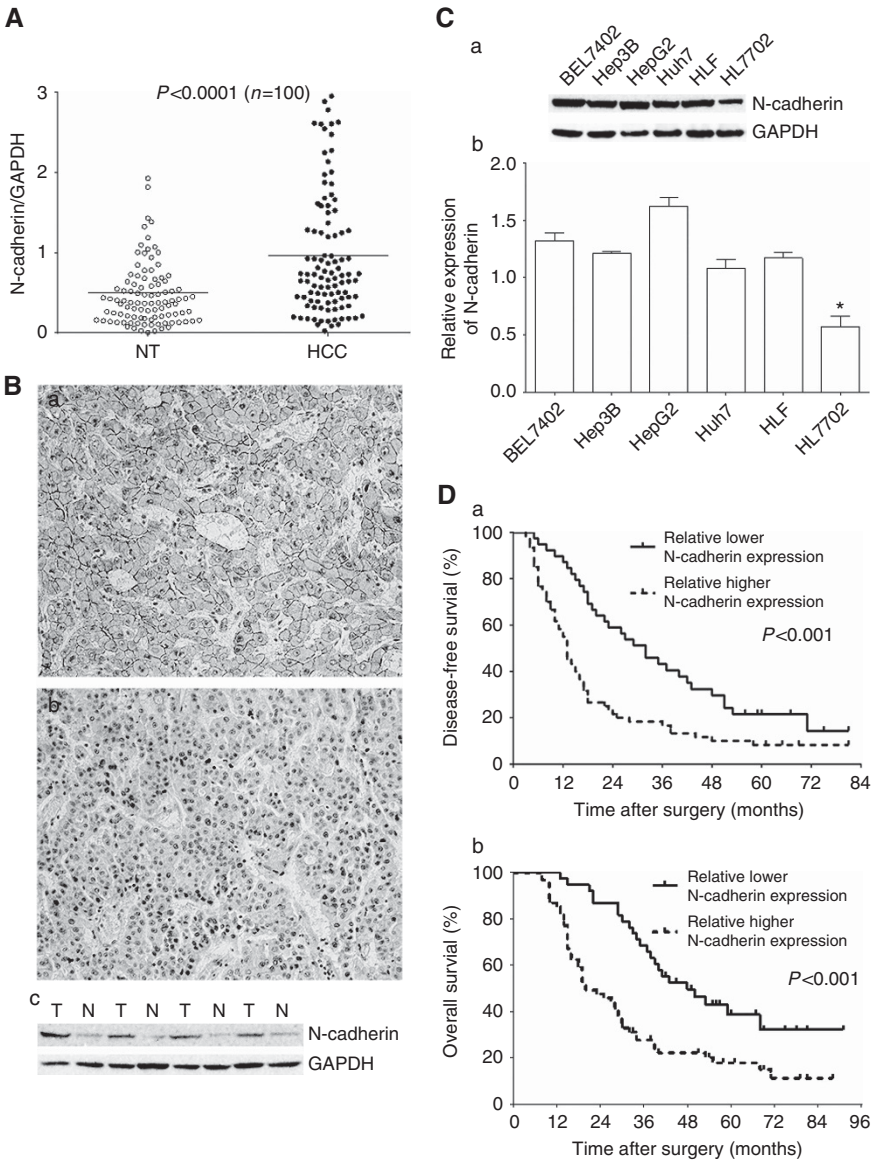

Figure 1. N-cadherin is overexpressed in HCC and is associated with the prognosis of HCC patients. (**A**) Relative expression levels of N-cadherin were detected using western blotting assay in 100 pairs of HCC patients' tumour tissues and corresponding adjacent liver tissues. (**B**) Representative images of N-cadherin expression in human HCC tissues (a) and corresponding adjacent liver tissues (b) were shown using immunohistochemical assay (× 100) and western blotting assay (c). High expression levels of N-cadherin were shown in HCC tissues and low expression levels of N-cadherin were exhibited in adjacent non-cancerous liver tissues. Membranous staining indicated positive staining for N-cadherin. (**C**) Relative expression levels of N-Cadherin in HCC cell lines were detected using western blotting assay. Histograms showed the relative expression of N-cadherin in HCC cell lines based on western blotting analysis. (**D**) The group of patients with high N-cadherin expression was significantly related to lower disease-free survival (a) and overall survival (b) rates after treated by curative resection for HCC. The asterisks indicate statistically significant changes (*$P < 0.05$).

lines and evaluated N-cadherin expression levels using western blotting analysis, which showed that miR-199b-5p induced the greatest decline of N-cadherin expression (Figure 2B).

Schematic representation of base pairing was observed between the seed sequence of mature miR-199b-5p and 3′-UTR of N-cadherin mRNA (Figure 2C). To further determine if N-cadherin was regulated by miR-199-5p, western blotting assays were conducted in HepG2 and Huh7 cells using different doses of miR-199b-5p mimics and miR-199b-5p inhibitors. Protein and mRNA expression levels of N-cadherin were reduced in miR-199b-5p overexpression HepG2 cells and were increased in miR-199b-5p downregulation Huh7 cells in a dose-dependent manner after transfection for 48 h ($P < 0.05$; Figure 2D). Moreover, HepG2 cells were transfected with miR-199b-5p inhibitor and Huh7 cells transfected with miR-199b-5p at different doses and controls. After transfection for 48 h, the protein and mRNA expression levels of N-cadherin were reduced in miR-199b-5p overexpression cells, and were increased in miR-199b-5p downregulation cells in a dose-dependent manner ($P < 0.05$; Supplementary Figure 1). Luciferase assay showed that miR-199b-5p suppressed luciferase expression of Luc-UTR and miR-199b-5p inhibitor promoted it but not the mutant, indicating that miR-199b-5p could directly target N-cadherin ($P < 0.05$; Figure 2E).

MiR-199b-5p is downregulated in HCC tissues and cell lines. To explore the potential role of miR-199b-5p in HCC, the expression profiles of miR-199b-5p were detected in the 100 paired HCC and adjacent liver tissues by qRT-PCR. Notably, miR-199b-5p

Table 1. The correlation between N-cadherin upregulation and clincopathological parameters in the patients with HCC

	N-cadherin expression level		
Clinicopathological variables	Upregulated ($n=61$)	Intact ($n=39$)	*P*-value
Age ($\leqslant 60$ *vs* >60) (years)	55 : 6	36 : 3	0.994
Gender (male/female)	51 : 10	36 : 3	0.241
HBV DNA ($\leqslant 10^5$ *vs* $>10^5$) (copies per ml)	44 : 17	32 : 7	0.257
Liver cirrhosis (absent *vs* present)	27 : 34	16 : 23	0.75
AFP ($\leqslant 400$ *vs* >400) (ng ml^{-1})	25 : 36	23 : 16	0.079
Histological grade (well/ moderate/poor)	2 : 30 : 29	5 : 30 : 4	<0.001*
Tumour size ($\leqslant 10$ *vs* >10 cm)	54 : 7	37 : 2	0.476
Tumour number (single *vs* multiple)	40 : 21	34 : 5	0.016*
Vascular invasion (absent *vs* present)	50 : 11	38 : 1	0.026*

Abbreviations: AFP = α-fetoprotein; HBV = hepatitis B virus; HCC = hepatocellular carcinoma. χ^2-test or the Fisher exact test; *statistically significant ($P<0.05$).

expression level was significantly decreased in HCC compared with para-tumour liver tissues, and low expression of miR-199b-5p was found in most HCC tissues (62%; Figure 3A). And downregulation of miR-199b-5p is inversely correlated with N-cadherin upregulation in HCC tissues ($P<0.0001$, Figure 3B). Moreover, HCC patients with low miR-199b-5p levels had a significantly shorter median DFS ($P<0.001$, Figure 3C) and OS ($P<0.0001$, Figure 3D) compared with those with high miR-199b-5p levels. Then we performed qRT-PCR assay to analyse miR-199b-5p expression in human HCC and normal liver cell lines. We found that the expression levels of miR-199b-5p were downregulated in HCC cells compared with normal liver cell line HL7702 ($P<0.05$, Figure 3E). And miR-199b-5p downregulation is inversely correlated with N-cadherin upregulation in HCC cells ($P<0.05$, Figure 3F). All the data indicate that miR-199b-5p functions as a tumour suppressor in HCC.

Overexpression of miR-199b-5p promotes cell aggregation, and inhibits migration and invasion, and N-cadherin restoration partly reverses the effect in HCC cells. To study the effects of miR-199b-5p on HCC cells, miR-199b-5p stably transfected and control clones were used for further experiments. The qRT-PCR analysis confirmed that miR-199b-5p stably transfected clones showed higher expression level of miR-199b-5p than those of control cells ($P<0.05$, Figure 4A), and N-cadherin expression levels were significantly reduced in miR-199b-5p stably transfected cells ($P<0.05$, Figure 4B).

Smaller cell aggregates were seen in control cells, while large cell aggregates were observed in miR-199b-5p overexpression cells, we found significantly increase in cell aggregation index in miR-199b-5p overexpression cells ($P<0.05$; Figure 4C). A wound-healing assay for cell migration was performed in miR-199b-5p and control clones of HepG2 and Huh7 cells. Expectedly, miR-199b-5p significantly decreased migration in both HCC cells ($P<0.05$; Figure 4D). In addition, the transwell chamber migration and invasion assay revealed that miR-199b-5p significantly reduced migration and invasion in both HCC cells ($P<0.05$; Figure 4E and F). Moreover, miR-199-5p and N-cadherin were co-transfected into HCC cells, the relative expression of miR-199b-5p and N-cadherin was shown in Figures 4G and 4H, respectively. We found that N-cadherin restoration partly reversed the effect of miR-199b-5p on cell aggregation, migration and invasion (Figure 4I–L).

To further investigate the growth inhibitory effect of miR-199b-5p in HCC cells, we performed CCK-8, colony formation, and anchorage-independent cell growth assays, showing that overexpression of miR-199b-5p did not significantly inhibited cell proliferation of HepG2 and Huh7 cells (Supplementary Figure 2A and B). Moreover, the cell cycle distribution and apoptosis analysis using flow cytometry indicated that miR-199b-5p did not significantly influence cell cycle progression or induce apoptosis in HCC cells (Supplementary Figure 2C and D).

TGF-β1 induced EMT and altered the expressions of miR-199b-5p and EMT markers in HCC cells. After TGF-β1 treatment for 48 h, HepG2 and Huh7 cells presented a fibroblast-like appearance (Supplementary Figure 3A), with N-cadherin expression detected by immunofluorescence staining significantly increased compared to those without TGF-β1 treatment (Supplementary Figure 3B). Meanwhile, the miR-199b-5p expression was remarkably reduced, along with expression of N-cadherin, p-Akt, Snail and Slug upregulated, and E-cadherin expression downregulated (Supplementary Figure 3C). Grey scale analysis was conducted based on the results of western blotting assay (Supplementary Figure 3D).

MiR-199b-5p attenuates TGF-β1 induced EMT in HCC. After TGF-β1 treatment for 48 h, HepG2 cells had cobblestone-like morphology in the miR-199b-5p overexpression group, and had fibroblast-like appearance in both control and N-cadherin overexpression group. Furthermore, we found that N-cadherin restoration in the miR-199b-5p overexpression group partially reversed the inhibitory effect of miR-199b-5p on EMT traits. Immunofluorescence staining showed that N-cadherin expression was remarkably reduced, while miR-199b-5p was transfected into HepG2 cells with TGF-β1 treatment for 48 h (Figure 5A) and miR-199b-5p was detected while N-cadherin, miR-199b-5p and the controls were co-transfected into TGF-β1-treated HepG2 cells (Figure 5B). It is also indicated that miR-199b-5p overexpression attenuated TGF-β1 induced EMT-related factors in HCC cells, and N-cadherin restoration partially promoted the p-Akt expression, but had little effect on expression of EMT-related factors using western blotting assay (Figure 5C) and grey scale analysis (Figure 5D).

MiR-199b-5p inhibits human HCC xenograft metastasis in nude mice. To examine whether miR-199b-5p could suppress metastatic features of HCC *in vivo*, intraperitoneal xenograft models were established with stably transfected miR-199b-5p and control HepG2 clones, which had been induced by TGF-β1 for 48 h. We found that miR-199b-5p could markedly inhibit the tumour metastasis *in vivo* (Figure 6A), which revealed markedly reduced tumour number derived from transfected miR-199b-5p cells (10.33 ± 4.04 *vs* 45 ± 8.89; $P<0.05$; Figure 6B). Then we explored the underlying mechanisms of tumour suppression induced by miR-199b-5p, immunohistochemical staining assay indicated that the EMT-associated factors induced by TGF-β1, especially N-cadherin and p-Akt, were markedly inactivated and E-cadherin expression was increased (Figure 6C and D).

TGF-β1 induced EMT through Akt signalling pathway in HCC. After TGF-β1 treatment without or with SB431542 for 48 h, HCC cells had fibroblast-like appearance in both groups (Supplementary Figure 4A), and immunofluorescence staining showed that N-cadherin expression was not significantly changed (Supplementary Figure 4B). Moreover, SB431542 did not significantly changed expression profiles of TGF-β1 induced EMT-related factors except Smad-dependent pathway in HCC cells (Supplementary Figure 4C). Thus, our data suggested that TGF-β1 induced EMT through non-Smad signalling pathway in HCC. We further utilised Akti VIII, a selective inhibitor of Akt1/2, to investigate the mechanisms of EMT. After TGF-β1 treatment

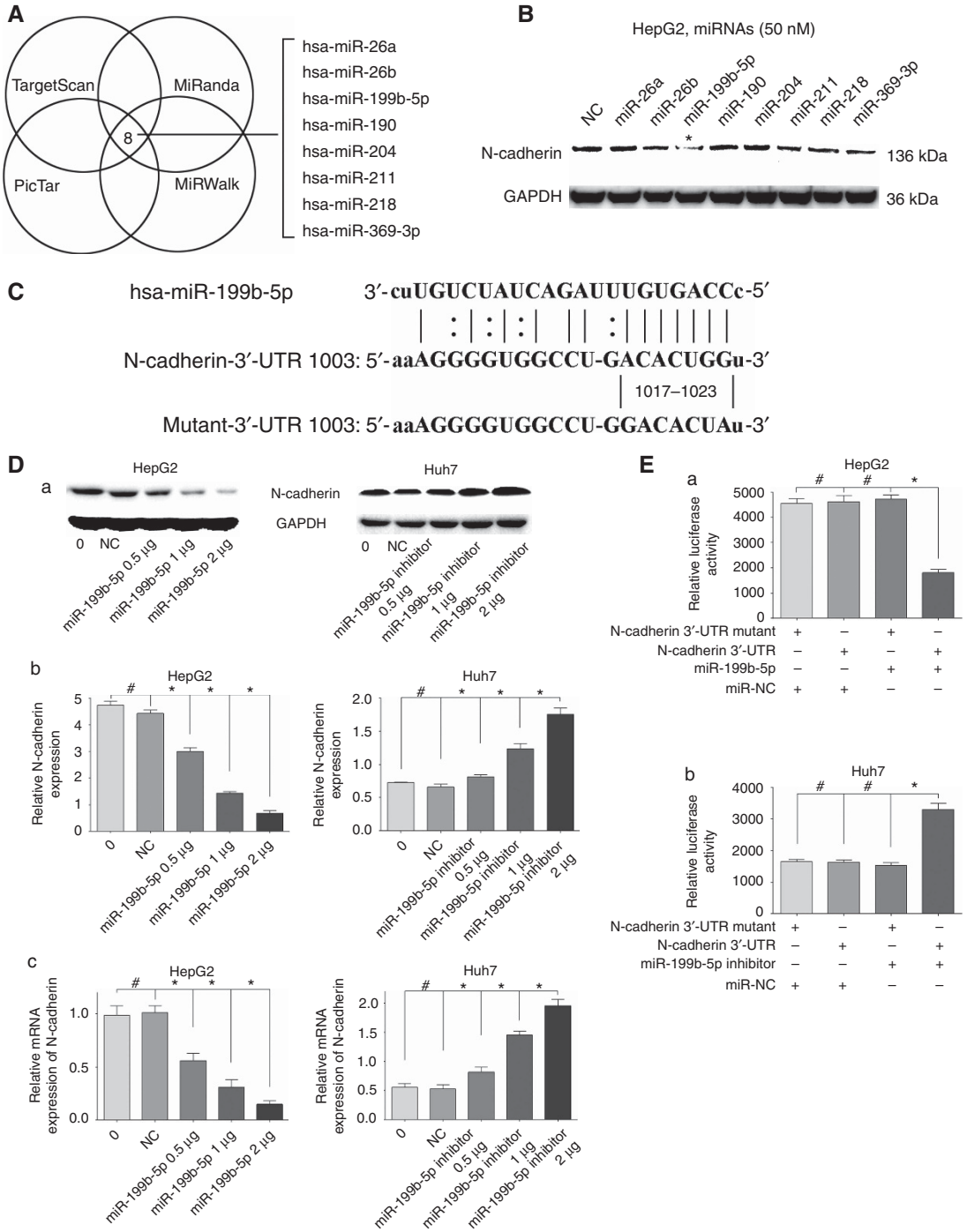

Figure 2. N-cadherin is a direct target of miR-199b-5p in HCC cells. (**A**) Venn diagram showed the overlap from four miRNA databases, identifying eight potential miRNAs targeting N-Cadherin mRNA. (**B**) Western blotting assay represented N-cadherin expression levels in the HepG2 cells transfected with eight miRNAs mimics and negative control (NC). GAPDH was used as the loading control. (**C**) Schematic diagram exhibited consequential pairing of miR-199b-5p and N-cadherin 3′-UTR predicted by miRanda database (http://www.microRNA.org). Mutant-3′-UTR indicated the 3′-UTR of N-Cadherin with the mutation in miR-199b-5p putative binding sites. (**D**) HepG2 cells were transfected with miR-199b-5p and Huh7 cells transfected with miR-199b-5p inhibitor at different doses and controls. After transfection for 48 h, the protein levels of N-Cadherin were examined by western blotting assay (a), the average grey scale intensities were measured by IPP 6.0 (b), and the mRNA levels of N-cadherin were examined by qRT-PCR (c). (**E**) Luciferase assay on HepG2 and Huh7 cells showed that miR-199b-5p markedly suppressed luciferase activity of wild-type reporter constructs in HepG2 cells (a), and miR-199b-5p inhibitor markedly increased luciferase activity of wild-type reporter constructs in Huh7 cells (b). $^{*}P < 0.05$, $^{\#}P > 0.05$.

without or with Akti VIII for 48 h, both HepG2 and Huh7 cells had fibroblast-like appearance in TGF-β1 without Akti VIII group, and cells had cobblestone-like morphology in TGF-β1 with Akti VIII group (Supplementary Figure 5A). Immunofluorescence staining showed that N-cadherin expression was significantly downregulated in TGF-β1 with Akti VIII group compared to TGF-β1 without Akti VIII group (Supplementary Figure 5B). What is more, expression of N-cadherin, and EMT-related factors was significantly changed in TGF-β1 with Akti VIII group compared to TGF-β1 without Akti VIII group (Supplementary Figure 5C).

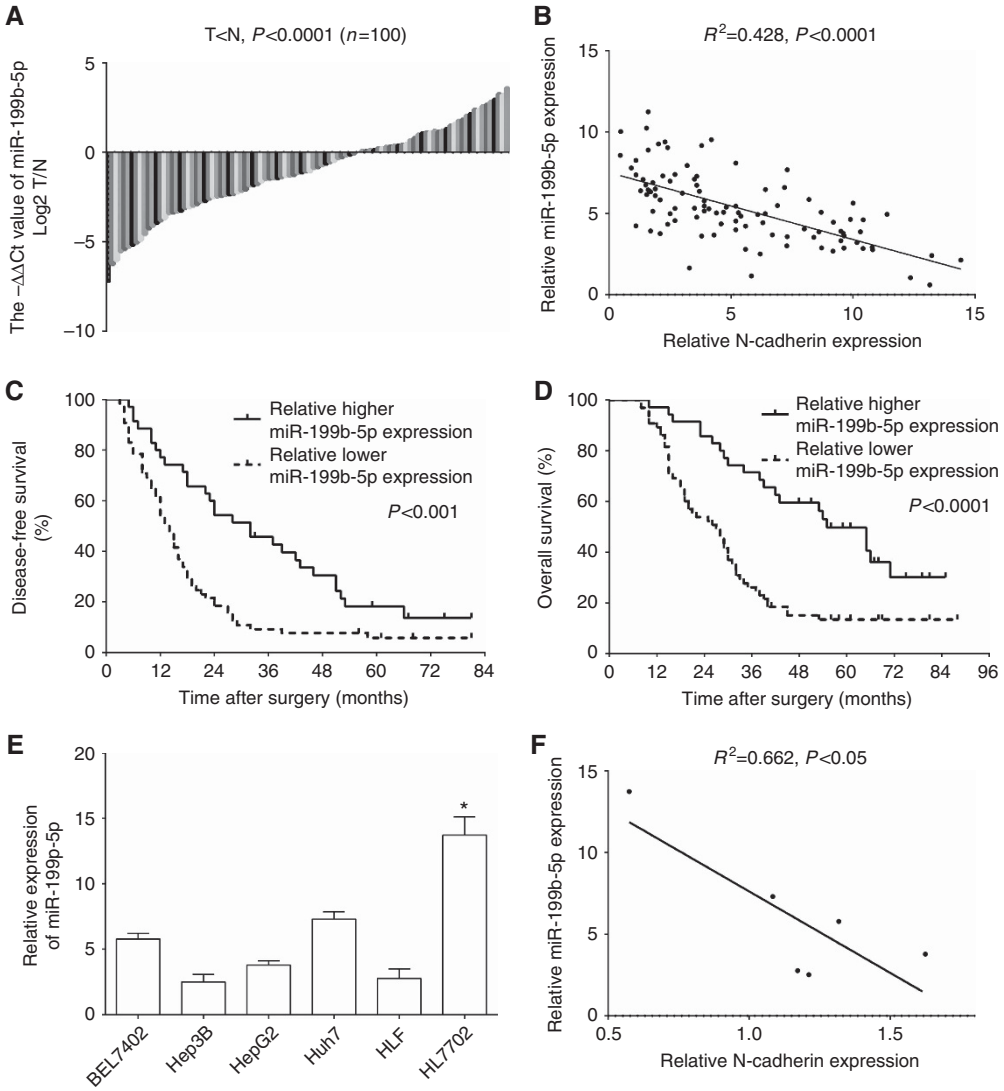

Figure 3. MiR-199b-5p is downregulated in HCC, and its downregulation is inversely correlated with the N-Cadherin overexpression. (**A**) MiR-199b-5p expression levels were significantly downregulated in HCC tissues compared with those of corresponding adjacent liver tissues ($n = 100$, $P < 0.0001$). Results were normalised to *RNU6B* gene. (**B**) Downregulation of miR-199b-5p is inversely correlated with N-cadherin upregulation in HCC ($R^2 = 0.428$, $P < 0.0001$, Pearson's correlation). Kaplan–Meier analysis estimated disease-free survival (**C**) and overall survival (**D**) in the HCC patients according to miR-199b-5p expression level. (**E**) MiR-199b-5p is downregulated in HCC cells, and its downregulation inversely correlated with the N-cadherin overexpression (**F**). *$P < 0.05$.

A regulatory loop exists between N-Cadherin and Akt in HCC cells. Since TGF-β1-induced EMT can be mediated through Akt signalling pathways, we explored the expression of N-cadherin and phosphorylation of Akt signalling in HCC cells. We found that miR-199b-5p could inhibit TGF-β1-activated Akt phosphorylation, and N-cadherin restoration partly reversed the effect (Figure 7A). In addition, we examined that knockdown of N-cadherin could also inhibit TGF-β1-activated Akt phosphorylation (Figure 7B). Meanwhile, we demonstrated that PI3K inhibitor (LY294002) blocked TGF-β1 induced N-cadherin overexpression (Figure 7C), and N-cadherin overexpression activated Akt signalling, while LY294002 caused N-Cadherin downregulation (Figure 7D). We further examined that Akti VIII blocked TGF-β1-induced N-cadherin overexpression, and N-cadherin siRNA in turn suppressed TGF-β1-induced Akt activation (Figure 7E). In addition, in the model of TGF-β1-induced HepG2 cells for 48 h, Akti VIII were added at different times. N-cadherin were not significantly changed when Akti VIII were added at early stage (at 0 h). However, N-cadherin significantly increased when Akti VIII were added in the next time points (at 6 h, 12 h and 24 h). It is indicated that TGF-β1 induces N-cadherin overexpression through Akt phosphorylation (Figure 7F). In the next model of TGF-β1-induced HepG2 cells for 48 h, N-cadherin siRNA were added at different times. The p-Akt expression significantly increased when N-Cadherin siRNA were added at early stage (at 0 h), and it further significantly increased when N-cadherin siRNA were added at late stage (at 12 h and 24 h) (Figure 7G). It has been indicated that TGF-β1 induces rapid activation of Akt at early stage. Our data found that reduction of N-cadherin could suppress the second wave of Akt activation at late stage, which indicated that TGF-β1-induced N-cadherin overexpression further promoted the second wave of Akt activation at late stage. In summary, the data suggest that a positive regulatory loop exists between N-cadherin and Akt signalling.

DISCUSSION

Cadherins are calcium-dependent cell adhesion molecules that involved in multiple cellular processes, and play important roles in

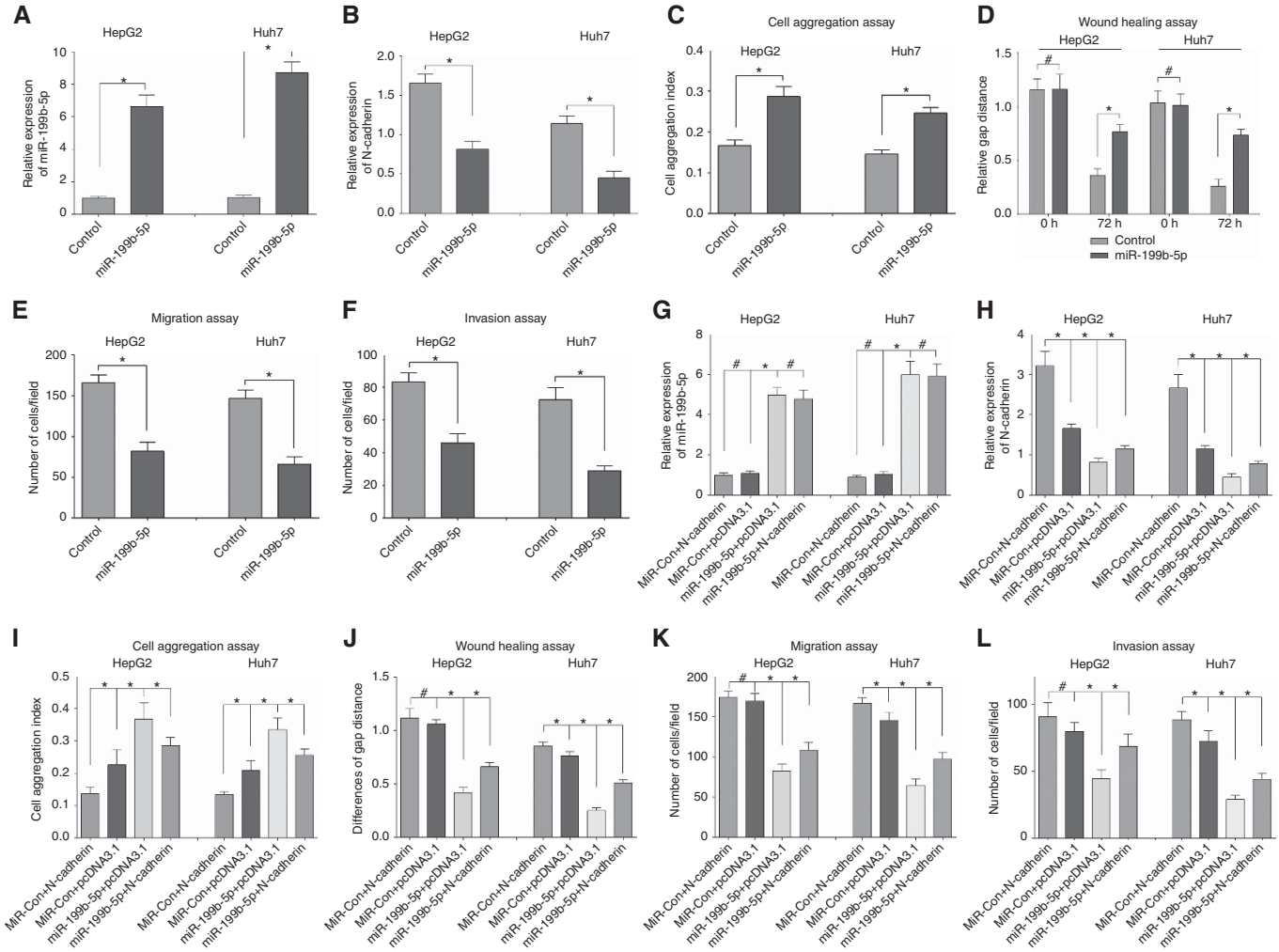

Figure 4. MiR-199b-5p promotes cell aggregation, suppresses cell migration and invasion in HCC cell lines, and N-Cadherin restoration partly reverses the effect. (**A**) Relative expression of miR-199b-5p was detected by qRT-PCR assay in HepG2 and Huh7 cell lines stably transfected with miR-199b-5p. (**B**) Relative expression of N-Cadherin was detected by western blotting assay in HepG2 and Huh7 cell lines stably transfected with miR-199b-5p. (**C**) MiR-199b-5p overexpression in HepG2 and Huh7 cells promotes homophilic cell aggregation. (**D**) Cell migration ability was evaluated by wound-healing assay measuring gap distance at time point 0 and 72 h. (**E**, **F**) Cell migration and invasion assay showed the number of cells across the membrane with 8 mm pores without or with Matrigel. In addition, expression of miR-199-5p (**G**) and N-cadherin (**H**) was detected while miR-199-5p and N-Cadherin were co-transfected into HCC cells. N-Cadherin restoration partly reversed the effect of miR-199b-5p on cell aggregation, migration and invasion (**I–L**). Each experiment was repeated three times. $^{*}P<0.05$, $^{\#}P>0.05$.

EMT, tumour invasion and metastasis (Jeanes *et al*, 2008; Maitre and Heisenberg, 2013). Unlike E-cadherin, which has been well established as a tumour suppressor gene in cancer, N-cadherin overexpression is reported to associate with heighted invasive potential in breast cancer, bladder cancer and pancreatic carcinoma (Nakajima *et al*, 2004; Nagi *et al*, 2005; Lascombe *et al*, 2006). In HCC, however, the role of N-cadherin still remains controversial. The study by Zhan *et al* (2012) suggested that reduced N-cadherin staining was significantly correlated with tumour differentiation and vascular invasion, and predicted a higher risk of recurrence after hepatectomy. However, Seo *et al* (2008) reported that N-cadherin was remarkably upregulated in HCC, and was associated with post-operative recurrence. Our results were consistent with Seo *et al* (2008), which found that N-cadherin was highly expressed in HCC tissues compared with that in adjacent liver tissues, and was significantly correlated with the tumour differentiation, multifocal tumours and vascular invasion. These data indicate that over-expressed N-cadherin contributed greatly to the invasion, metastasis and recurrence of HCC.

Many studies have shown that miRNAs behave as a ubiquitous feature by post-transcriptionally inhibiting target genes (Asangani *et al*, 2008; Aqeilan *et al*, 2010). To investigate whether miRNAs dysfunction were involved in the mechanism of N-Cadherin overexpression in HCC, we utilised four miRNA databases to scan for potential miRNAs that target N-cadherin 3′-UTR. We subsequently identified that hsa-miR-199b-5p could significantly suppress N-cadherin expression in HCC cells. It has been reported that reduced miR-199b-5p expression was correlated with poor prognosis of breast cancer patients, and miR-199b-5p inhibited HER2 expression in breast cancer cells (Fang *et al*, 2013, 2016). Favreau *et al* found that miR-199b-5p was downregulated and targeted PODXL and DDR1 in acute myeloid leukaemia (Favreau *et al*, 2012). Chiu LY *et al* reported that miR-199b-5p was significantly downregulated in HCC cell lines using massively parallel sequencing (Chiu *et al*, 2014). Until now, limited information is available about the role of miR-199b-5p in HCC. Therefore, the role of miR-199b-5p was further explored in this paper. We determined that miR-199b-5p levels were markedly decreased in HCC tissues and HCC cell lines by comparison with para-tumour liver tissues and normal liver cells (Figure 1A), suggesting that miR-199b-5p could be a useful diagnostic biomarker in HCC. Moreover, miR-199b-5p overexpression in

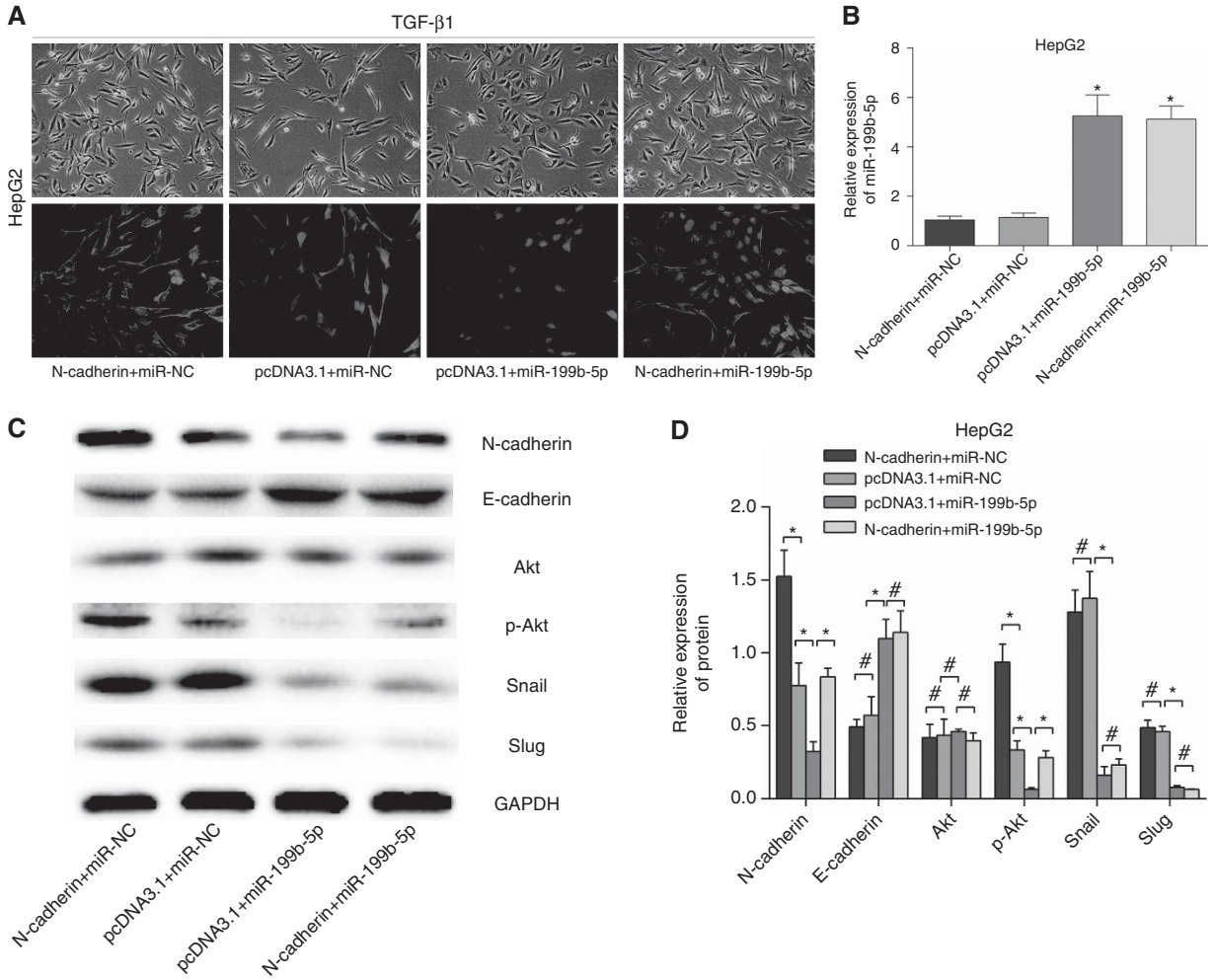

Figure 5. MiR-199b-5p overexpression attenuates the TGF-β1 induced EMT phenotype, and N-Cadherin overexpression rescues the TGF-β1 induced EMT phenotype. (**A**) Treatment of co-transfected HepG2 cells by TGF-β1. Morphological appearance and immunofluorescence staining of N-cadherin expression of the cells were shown ($\times$ 100). The influences of TGF-β1 treatment on the expressions of miR-199b-5p, N-cadherin and EMT-related factors in co-transfected HepG2 cells. The expression of miR-199b-5p was detected by qRT-PCR assay (**B**), and the expressions of N-cadherin and EMT-related factors were evaluated by western blotting assay (**C**) and grey scale analysis (**D**). $^{*}P<0.05$, $^{\#}P>0.05$.

HCC cells induced cell aggregation, reduced cell migration and invasion, and suppress TGF-β1-induced EMT *in vitro*. *In vivo* experiment also indicated that miR-199b-5p overexpression inhibited HCC cell metastasis. All the evidences revealed that miR-199b-5p functions as a tumour suppressor in HCC.

With loss of E-cadherin and upregulation of N-cadherin, EMT is considered to be the important mechanisms regulating the progression for the invasive behaviour of cancer cells, such as promotion of cell detachment, migration and vascular invasion. TGF-β1 has been regarded as the most effective inductor for EMT. However, the mechanism of TGF-β1 induced EMT and carcinogenesis in HCC are not yet well established. Recent studies have reported that miRNAs was involved in TGF-β1-mediated EMT to modulate the cell migration, invasion and extracellular matrix degradation. Zhou *et al* (2015) demonstrated that miR-125b attenuated EMT via targeting Smad2 and Smad4 in HCC. Li *et al* (2016) reported that miR-21 could promote TGF-β signalling to induce EMT through upregulating PTEN expression in gastric cancer. Zhang *et al* (2016) indicated that miR-29c overexpression could repress the Sp1/TGF-β axis-induced EMT in lung cancer. In this study, we showed that the TGF-β1-induced EMT was suppressed through the miR-199b-5p/N-cadherin axis. Moreover, we found that miR-199b-5p inhibited metastasis *in vivo*. Our data also indicated that TGF-β1 induced EMT and miR-199b-5p downregulation through non-Smad signalling pathways. Further studies need to illustrate the mechanisms of TGF-β1-induced miR-199b-5p downregulation.

It has been indicated that the activated PI3K/Akt signalling has a pivotal role in TGF-β1-induced EMT (Meadows *et al*, 2009; Yan *et al*, 2009). Li *et al* (2016) found that miR-21 promoted phosphorylation of Akt through downregulating PTEN in TGF-β1-mediated EMT model in gastric cancer. Wu *et al* (2011) suggested that TGF-β1 regulated PI3K/Akt pathway promoting the activity of Snail, Slug and CD147 signalling cascade, and then induced EMT in HCC. Augustine *et al* (2008) showed that ADH-1, a N-cadherin antagonist which disrupts cell adhesion, enhanced antitumour effects of chemotherapy in melanoma and increased p-Akt. TGF-β1-Akt signalling-N-cadherin axis has been successfully verified in many studies; however, whether N-cadherin influences downstream signalling pathway needs further investigation. Interestingly, we found that N-cadherin siRNA or miR-199b-5p suppressed TGF-β1-activated Akt phosphorylation in HCC cells. It has been indicated that TGF-β1 induces rapid activation of Akt within 30 min and followed by a second wave of activation at late stage (Bakin *et al*, 2000; Zhang, 2009). Our data found that knockdown of N-cadherin could suppress the second wave of Akt activation, which suggested that TGF-β1-induced N-cadherin

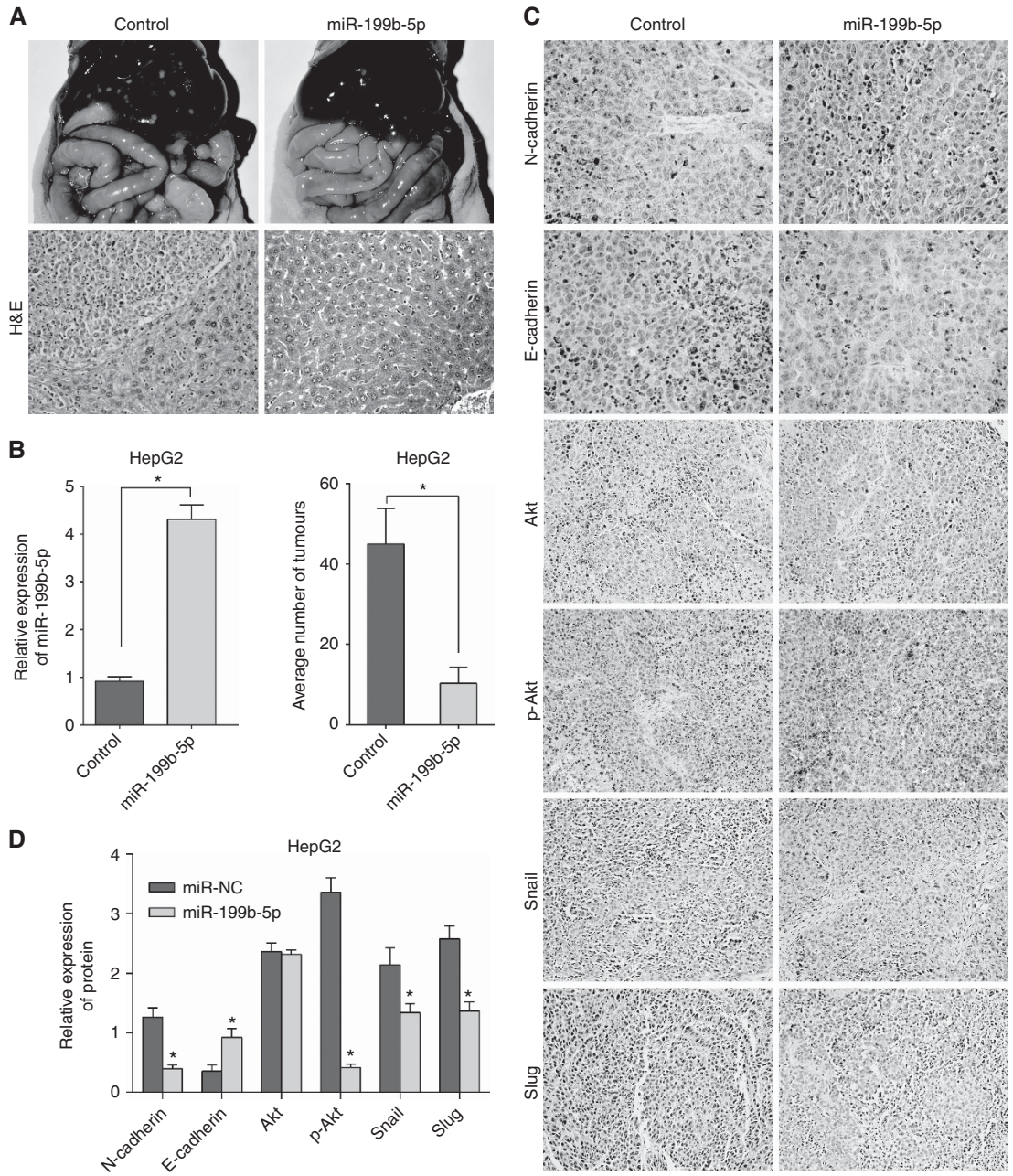

Figure 6. MiR-199b-5p attenuates EMT-associated traits of HCC cells *in vivo*. (**A**) The tumours derived from the TGF-β1 treated HepG2 miR-199b-5p overexpression cell clones were less in number than the TGF-β1 treated HepG2 control cell clones ($n=5$ each group). Representative H&E staining of the tumours was shown. (**B**) MiR-199b-5p expression status and the number of the xenograft tumour tissues in both groups were detected. (**C**) The expression status of N-Cadherin and EMT-related factors of the xenograft tumour tissues in both groups were determined. (**D**) The average grey scale intensities were measured by IPP 6.0. *$P<0.05$.

overexpression promoted the second wave of Akt activation. The positive regulatory loop between N-cadherin and Akt signalling needs further investigation to unveil the mechanisms of TGF-β1-mediated EMT in HCC cells.

In conclusion, N-cadherin was markedly overexpressed and miR-199b-5p was significantly downregulated in HCC. MiR-199b-5p promotes cell aggregation, suppresses cell migration and invasion and inhibits TGF-β1-induced EMT in HCC. TGF-β1-induced N-cadherin overexpression promoted the second wave of Akt activation at late stage and a positive regulatory loop between N-cadherin and Akt signalling was demonstrated as a novel mechanism of TGF-β1-mediated EMT in HCC cells.

ACKNOWLEDGEMENTS

We thank Professor Zhi-yong Huang for guidance of the study. This work was supported by the National Natural Science Foundation of China (81202300 and 81172293).

CONFLICT OF INTEREST

The authors declare no conflict of interest.

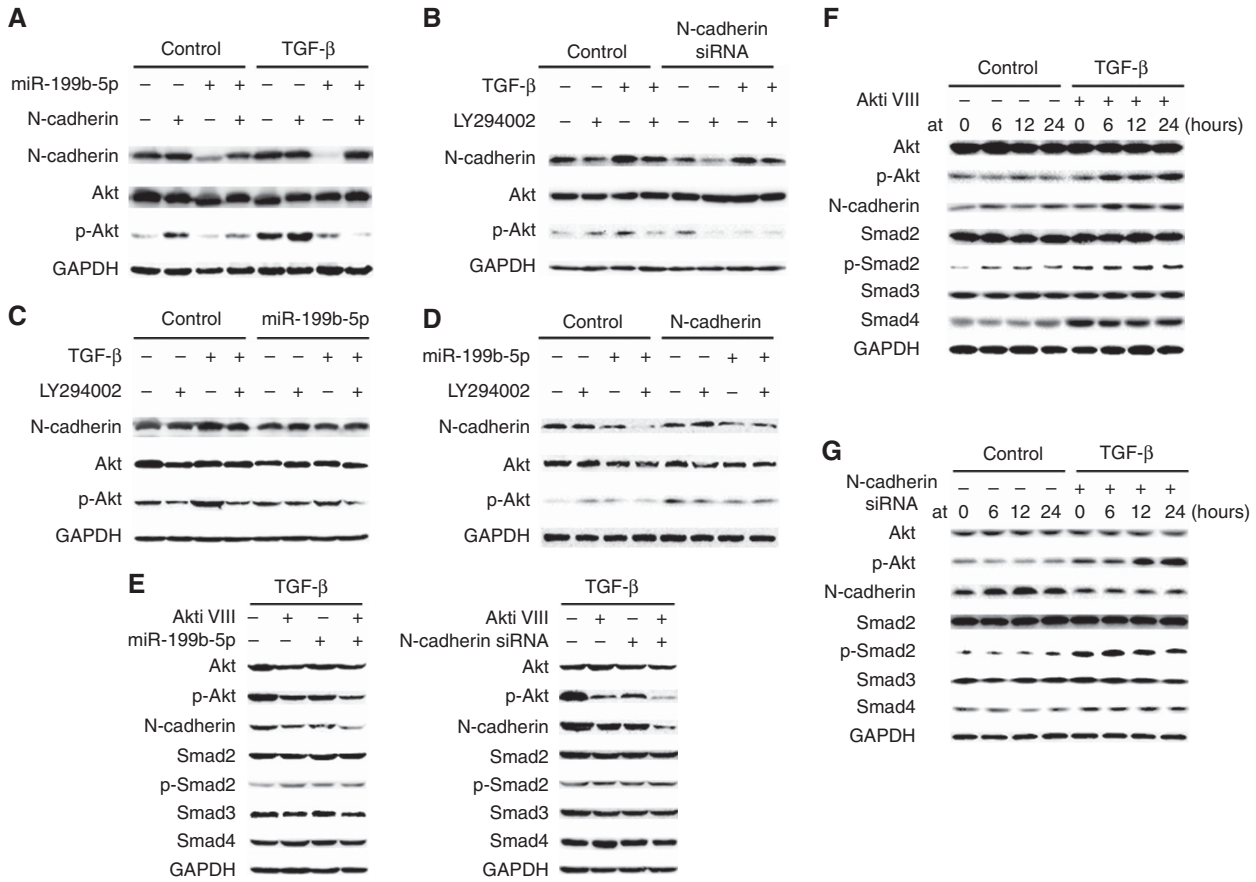

Figure 7. A regulatory loop exists between N-cadherin and Akt in HCC cells. (**A**) MiR-199b-5p inhibited TGF-β1 induced Akt signalling activation, and N-cadherin restoration partly reversed the effect. (**B**) PI3K inhibitor (LY294002) blocked TGF-β1 induced N-cadherin overexpression. (**C**) MiR-199b-5p inhibited N-cadherin expression, and TGF-β1 partly reversed the effect. (**D**) N-Cadherin overexpression activated Akt signalling and LY294002 downregulated N-cadherin expression. (**E**) Akti VIII blocked TGF-β1 induced N-cadherin overexpression, and N-cadherin siRNA in turn suppressed TGF-β1 induced Akt activation. (**F**) In the model of TGF-β1 induced HepG2 cell for 48 h, Akti VIII were added at different times. N-cadherin were not significantly changed when Akti VIII were added at early stage (at 0 h). However, N-cadherin expression significantly increased when Akti VIII were added in the next time points (at 6 h, 12 h and 24 h). (**G**) In the next model of TGF-β1 induced HepG2 cell for 48 h, N-cadherin siRNA were added at different times. The p-Akt expression significantly increased when N-cadherin siRNA were added at early stage (at 0 h), and it further significantly increased when N-cadherin siRNA were added at late stage (at 12 h and 24 h). All of the experiments were performed in triplicate.

AUTHOR CONTRIBUTIONS

(1) Conception and design of the study: S-j Zhou, F-y Liu and H-f Liang. (2) Acquisition, analysis and interpretation of data: S-j Zhou, A-h Zhang, Y Wang, R Ma. (3) Drafting and revising the article: S-j Zhou, Y-h Jiang, N-f Sun. (4) Final approval of the version to be submitted: all authors.

REFERENCES

Aqeilan RI, Calin GA, Croce CM (2010) miR-15a and miR-16-1 in cancer: discovery, function and future perspectives. *Cell Death Differ* **17**(2): 215–220.

Asangani IA, Rasheed SA, Nikolova DA, Leupold JH, Colburn NH, Post S, Allgayer H (2008) MicroRNA-21 (miR-21) post-transcriptionally downregulates tumour suppressor Pdcd4 and stimulates invasion, intravasation and metastasis in colorectal cancer. *Oncogene* **27**(15): 2128–2136.

Augustine CK, Yoshimoto Y, Gupta M, Zipfel PA, Selim MA, Febbo P, Pendergast AM, Peters WP, Tyler DS (2008) Targeting N-cadherin enhances antitumor activity of cytotoxic therapies in melanoma treatment. *Cancer Res* **68**(10): 3777–3784.

Bakin AV, Tomlinson AK, Bhowmick NA, Moses HL, Arteaga CL (2000) Phosphatidylinositol 3-kinase function is required for transforming growth factor beta-mediated epithelial to mesenchymal transition and cell migration. *J Biol Chem* **275**(47): 36803–36810.

Bremnes RM, Veve R, Gabrielson E, Hirsch FR, Baron A, Bemis L, Gemmill RM, Drabkin HA, Franklin WA (2002) High-throughput tissue microarray analysis used to evaluate biology and prognostic significance of the E-cadherin pathway in non-small-cell lung cancer. *J Clin Oncol* **20**(10): 2417–2428.

Calin GA, Croce CM (2006) MicroRNA signatures in human cancers. *Nat Rev Cancer* **6**(11): 857–866.

Chen WX, Zhang ZG, Ding ZY, Liang HF, Song J, Tan XL, Wu JJ, Li GZ, Zeng Z, Zhang BX, Chen XP (2016) MicroRNA-630 suppresses tumour metastasis through the TGF-beta- miR-630-Slug signaling pathway and correlates inversely with poor prognosis in hepatocellular carcinoma. *Oncotarget* **7**(16): 22674–22686.

Chiu LY, Kishnani PS, Chuang TP, Tang CY, Liu CY, Bali D, Koeberl D, Austin S, Boyette K, Weinstein DA, Murphy E, Yao A, Chen YT, Li LH (2014) Identification of differentially expressed microRNAs in human hepatocellular adenoma associated with type I glycogen storage disease: a potential utility as biomarkers. *J Gastroenterol* **49**(8): 1274–1284.

Croce CM (2009) Causes and consequences of microRNA dysregulation in cancer. *Nat Rev Genet* **10**(10): 704–714.

Dweep H, Sticht C, Pandey P, Gretz N (2011) miRWalk–database: prediction of possible miRNA binding sites by 'walking' the genes of three genomes. *J Biomed Inform* **44**(5): 839–847.

El-Serag HB, Marrero JA, Rudolph L, Reddy KR (2008) Diagnosis and treatment of hepatocellular carcinoma. *Gastroenterology* **134**(6): 1752–1763.

El-Serag HB, Rudolph KL (2007) Hepatocellular carcinoma: epidemiology and molecular carcinogenesis. *Gastroenterology* **132**(7): 2557–2576.

Fang C, Wang FB, Li Y, Zeng XT (2016) Down-regulation of miR-199b-5p is correlated with poor prognosis for breast cancer patients. *Biomed Pharmacother* **84**: 1189–1193.

Fang C, Zhao Y, Guo B (2013) MiR-199b-5p targets HER2 in breast cancer cells. *J Cell Biochem* **114**(7): 1457–1463.

Favreau AJ, Cross EL, Sathyanarayana P (2012) miR-199b-5p directly targets PODXL and DDR1 and decreased levels of miR-199b-5p correlate with elevated expressions of PODXL and DDR1 in acute myeloid leukemia. *Am J Hematol* **87**(4): 442–446.

Gravdal K, Halvorsen OJ, Haukaas SA, Akslen LA (2007) A switch from E-cadherin to N-cadherin expression indicates epithelial to mesenchymal transition and is of strong and independent importance for the progress of prostate cancer. *Clin Cancer Res* **13**(23): 7003–7011.

Hanahan D, Weinberg RA (2011) Hallmarks of cancer: the next generation. *Cell* **144**(5): 646–674.

Hazan RB, Phillips GR, Qiao RF, Norton L, Aaronson SA (2000) Exogenous expression of N-cadherin in breast cancer cells induces cell migration, invasion, and metastasis. *J Cell Biol* **148**(4): 779–790.

Huang ZY, Wu Y, Hedrick N, Gutmann DH (2003) T-cadherin-mediated cell growth regulation involves G2 phase arrest and requires p21(CIP1/WAF1) expression. *Mol Cell Biol* **23**(2): 566–578.

Jeanes A, Gottardi CJ, Yap AS (2008) Cadherins and cancer: how does cadherin dysfunction promote tumour progression? *Oncogene* **27**(55): 6920–6929.

Kim VN (2005) MicroRNA biogenesis: coordinated cropping and dicing. *Nat Rev Mol Cell Biol* **6**(5): 376–385.

Lamouille S, Xu J, Derynck R (2014) Molecular mechanisms of epithelial-mesenchymal transition. *Nat Rev Mol Cell Biol* **15**(3): 178–196.

Lascombe I, Clairotte A, Fauconnet S, Bernardini S, Wallerand H, Kantelip B, Bittard H (2006) N-cadherin as a novel prognostic marker of progression in superficial urothelial tumours. *Clin Cancer Res* **12**(9): 2780–2787.

Li C, Song L, Zhang Z, Bai XX, Cui MF, Ma LJ (2016) MicroRNA-21 promotes TGF-beta1-induced epithelial-mesenchymal transition in gastric cancer through up-regulating PTEN expression. *Oncotarget* **7**(41): 66989–67003.

Li G, Satyamoorthy K, Herlyn M (2001) N-cadherin-mediated intercellular interactions promote survival and migration of melanoma cells. *Cancer Res* **61**(9): 3819–3825.

Liu FY, Zhou SJ, Deng YL, Zhang ZY, Zhang EL, Wu ZB, Huang ZY, Chen XP (2015) MiR-216b is involved in pathogenesis and progression of hepatocellular carcinoma through HBx-miR-216b-IGF2BP2 signaling pathway. *Cell Death Dis* **6**: e1670.

Maitre JL, Heisenberg CP (2013) Three functions of cadherins in cell adhesion. *Curr Biol* **23**(14): R626–R633.

Meadows KN, Iyer S, Stevens MV, Wang D, Shechter S, Perruzzi C, Camenisch TD, Benjamin LE (2009) Akt promotes endocardial-mesenchyme transition. *J Angiogenes Res* **1**: 2.

Nagi C, Guttman M, Jaffer S, Qiao R, Keren R, Triana A, Li M, Godbold J, Bleiweiss IJ, Hazan RB (2005) N-cadherin expression in breast cancer: correlation with an aggressive histologic variant–invasive micropapillary carcinoma. *Breast Cancer Res Treat* **94**(3): 225–235.

Nakajima S, Doi R, Toyoda E, Tsuji S, Wada M, Koizumi M, Tulachan SS, Ito D, Kami K, Mori T, Kawaguchi Y, Fujimoto K, Hosotani R, Imamura M (2004) N-cadherin expression and epithelial-mesenchymal transition in pancreatic carcinoma. *Clin Cancer Res* **10**(12 Pt 1): 4125–4133.

Nass SJ, Herman JG, Gabrielson E, Iversen PW, Parl FF, Davidson NE, Graff JR (2000) Aberrant methylation of the estrogen receptor and E-cadherin 5' CpG islands increases with malignant progression in human breast cancer. *Cancer Res* **60**(16): 4346–4348.

Nieto MA, Huang RY, Jackson RA, Thiery JP (2016) Emt: 2016. *Cell* **166**(1): 21–45.

Seo DD, Lee HC, Kim HJ, Min HJ, Kim KM, Lim YS, Chung YH, Lee YS, Suh DJ, Yu E, Chun SY (2008) Neural cadherin overexpression is a predictive marker for early postoperative recurrence in hepatocellular carcinoma patients. *J Gastroenterol Hepatol* **23**(7 Pt 1): 1112–1118.

Umbas R, Isaacs WB, Bringuier PP, Schaafsma HE, Karthaus HF, Oosterhof GO, Debruyne FM, Schalken JA (1994) Decreased E-cadherin expression is associated with poor prognosis in patients with prostate cancer. *Cancer Res* **54**(14): 3929–3933.

Wang X, Chen X, Meng Q, Jing H, Lu H, Yang Y, Cai L, Zhao Y (2015) MiR-181b regulates cisplatin chemosensitivity and metastasis by targeting TGFbetaR1/Smad signaling pathway in NSCLC. *Sci Rep* **5**: 17618.

Wu J, Ru NY, Zhang Y, Li Y, Wei D, Ren Z, Huang XF, Chen ZN, Bian H (2011) HAb18G/CD147 promotes epithelial-mesenchymal transition through TGF-beta signaling and is transcriptionally regulated by Slug. *Oncogene* **30**(43): 4410–4427.

Yan W, Fu Y, Tian D, Liao J, Liu M, Wang B, Xia L, Zhu Q, Luo M (2009) PI3 kinase/Akt signaling mediates epithelial-mesenchymal transition in hypoxic hepatocellular carcinoma cells. *Biochem Biophys Res Commun* **382**(3): 631–636.

Zhan DQ, Wei S, Liu C, Liang BY, Ji GB, Chen XP, Xiong M, Huang ZY (2012) Reduced N-cadherin expression is associated with metastatic potential and poor surgical outcomes of hepatocellular carcinoma. *J Gastroenterol Hepatol* **27**(1): 173–180.

Zhang HW, Wang EW, Li LX, Yi SH, Li LC, Xu FL, Wang DL, Wu YZ, Nian WQ (2016) A regulatory loop involving miR-29c and Sp1 elevates the TGF-beta1 mediated epithelial-to-mesenchymal transition in lung cancer. *Oncotarget* **7**(52): 85905–85916.

Zhang YE (2009) Non-Smad pathways in TGF-beta signaling. *Cell Res* **19**(1): 128–139.

Zhou JN, Zeng Q, Wang HY, Zhang B, Li ST, Nan X, Cao N, Fu CJ, Yan XL, Jia YL, Wang JX, Zhao AH, Li ZW, Li YH, Xie XY, Zhang XM, Dong Y, Xu YC, He LJ, Yue W, Pei XT (2015) MicroRNA-125b attenuates epithelial-mesenchymal transitions and targets stem-like liver cancer cells through small mothers against decapentaplegic 2 and 4. *Hepatology* **62**(3): 801–815.

Supplementary Information accompanies this paper on British Journal of Cancer website (http://www.nature.com/bjc)